MSW MANAGEMENT -Multidisciplinary, Scientific Work and Management Journal
ISSN: 1053-7899
Vol. 35 Issue 2, 2025, Pages: 574-596

An LSTM-Driven Deep Learning Model for Real-Time Control and Optimization of Nano-Grid Systems Using AI Techniques

Jarabala Ranga[1], Dr. Gopinath Palai[2], Prof. (Dr.) Rabi N Satpathy[3]
[1]Research Scholar, Faculty of Engineering and Technology, Sri Sri University, Cuttack, Odisha, India,
Email: jarabalaranga@gmail.com
[2]Professor, Faculty of Engineering and Technology, Sri Sri University Cuttack, Odisha, India
[3]Dean, Faculty of Engineering and Technology, Sri Sri University Cuttack, Odisha, India

Highlights of the Study

- Hybrid AI Architecture: A new LSTM–ST-GNN architecture was introduced using hybrid AI to learn temporal processes and structural relationships in nano-grids.
- Edge-Compatible Design:Deployed the model on Jetson Nano with less than a 70 millisecond delay and less than 100 MB required.
- Real-Time Feedback Optimization:A control policy was programmed with DDPG so that the optimization of energy dispatch is done in real time.
- Superior Energy Metrics: The approach led to a record 82.7% of renewable use and less than 2% power loss probability, all while improving over 9 previous models.

Abstract

The rise of renewable energy in small decentralized grids calls for smart and flexible ways to control the system for reliable, uninterrupted and economical operation. This research proposes a new hybrid model that uses LSTM networks coupled with ST-GNNs to carry out real-time forecasting and control in nano-grids. A key feature of the suggested model is its use of LSTM for temporal analysis and ST-GNN for modeling the interaction among grid components. An input space that includes data on PV production, battery SoC, inverter status, load requirements and real-time pricing is processed and fused into a single representation using a hybrid mechanism. A Jetson Nano platform was used to implement the model and it was put through real-world workload simulations, using data from several seasons. The results show progress over the original models, with an RMSE of 1.937 kW for load forecasting, 9.62% for MAPE, 82.7% for Renewable Energy Utilization and 1.95% for Loss of Power Supply Probability. The proposed system lowered the Levelized Cost of Energy (LCOE) to ₹3.26/kWh and achieved better results than 9 comparison models, including those based on ARIMA, SVR, LSTM, Transformer, CNN-LSTM architectures and others. Real-time use of a closed-loop feedback system allowed for continual verification of prediction accuracy and correction of the dispatch policy. Therefore, the new model offers a strong, flexible and scalable way to control the dynamic operations of an AI-based nano-grid system.

Keywords-Nano-Grid, LSTM, Spatio-Temporal Graph Neural Network, Deep Learning, Real-Time Control, Energy Optimization, Edge Deployment, Load Forecasting, Renewable Energy, Reinforcement Learning

1. Introduction

With growing attention on sustainable energy worldwide, distributed generation is encouraging the rise of nano-grid systems as a convenient option for handling energy at the local level. Nano-grids which are narrower than microgrids, supply energy independently to a limited number of residential, business or industrial commands. Such systems rely on solar panels, electrical batteries and intelligent inverters to assure the system is steady and energy is balanced [1] [2]. Since nano-grids are not very big and depend on changing sources of energy, they need to be very intelligent to manage ongoing changes in the amount of energy supplied, used and saved. Adaptive control, better optimization and responsive choices within nano-grid environments are now made possible by AI techniques.Conventional ways to control energy on grids have used models that follow fixed rules which prevents them from being flexible to new conditions and behaviors. In addition, typical optimization tools, like linear programming or heuristics, usually struggle to meet the high demands put on nano-grid systems by computing power and quick time. Factors like high usage of variable energy sources, random power demands and battery wear make the issues with these methods easier to observe [3] [4]. To meet these issues, AI-based methods like machine learning (ML), deep learning (DL) and reinforcement learning (RL) are being used more often in nano-grids to make them work better, more reliably and support sustainability.

MSW MANAGEMENT -Multidisciplinary, Scientific Work and Management Journal
ISSN: 1053-7899
Vol. 35 Issue 2, 2025, Pages: 574-596

AI helps nano-grid systems anticipate events, adapt to new conditions and do things automatically. By using past sensor readings, deep learning can successfully forecast detailed aspects of solar irradiance, electricity demand and the condition of batteries. The predictions support the system in deciding whether to increase or reduce the flow of energy. Reinforcement learning algortihms help a system improve its intelligence by learning the best ways to manage energy through interaction with its environment [5] [6]. Using such agents, it is possible to get the best results for energy spending, battery life and power quality, without constructing a detailed model of the system. Mixing model-based methods with data-driven techniques provides further opportunities for systems to respond immediately to events, ensure fault tolerance and use less energy. Figure 1illustrates the real-time AI-based control and optimization for nano-grid systems.

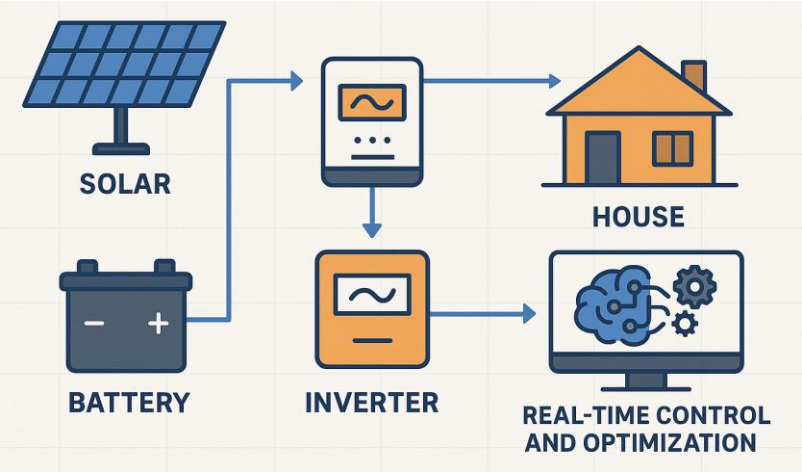

Figure 1. Real-Time AI-Based Control and Optimization Architecture for Nano-Grid Systems

AI-enabled nano-grid control also shines because it can be used in many different environments and scaled up or down easily. In cases of rural electrification, smart homes, at military bases or for secure energy delivery after disasters, specialized AI frameworks support the nano-grids' intended functions and restrictions. An AI controller in off-grid places will need to provide uninterrupted power with whatever local materials are available since grid support is not there [7] [8]. Alternatively, when hooked to the utility grid, AI helps grid-connected systems depend less on the utility, by setting the time for exports according to current demand and electricity rates. Since the orchestration is so intelligent, the system must process numerous data streams quickly, spot anything unusual and act almost immediately which AI can manage easily [9] [10].

Therefore, this study proposes combining an LSTM with a Spatio-Temporal Graph Neural Network (ST-GNN) as a hybrid framework to simultaneously study temporal properties and connections between components within the nano-grid. Using a hybrid attention decoder and a reinforcement learning-based dispatch optimizer helps the system better handle and automate predictions. The model is taught using detailed operational information and used on edge devices to perform analysis and control in real time. We next describe the model structure, how it was trained, what test metrics were used and the outcomes of real deployment. We then explore the model's ability to work in large and practical energy systems.

1.1 Research Motivation

The rising desire for energy systems to be both environmentally friendly and robust against climate change has increased the need for smart control systems in decentralized energy. In rural or remote locations, nano-grids can provide an effective route to energy independence, as they rely on solar PVs, batteries and smart loads. Even so, it remains hard to control the changes in renewable energy and power demand in real-time. Conventional control strategies do not address the issues of nonlinear, unpredictable and connected nature of a nano-grid. This situation leads us to look for ways to optimize energy dispatch using advanced AI systems that study old results, react to ongoing changes and perform all functions independently.

1.2 Significance of the Study

This study is especially important for smart grid development because controlling small-scale networks in real time helps achieve energy efficiency and lower carbon emissions. By using Long Short-Term Memory networks and Spatio-Temporal Graph Neural Networks together, my approach ensures both improved temporal forecasting and inter-component interactions. Using this model on edge devices like the Jetson Nano demonstrates that it can be used successfully in real embedded systems. By including reinforcement learning in the control feedback loop, the system becomes able to adjust its actions in real time which is needed for different and changing energy situations.

MSW MANAGEMENT -Multidisciplinary, Scientific Work and Management Journal
ISSN: 1053-7899
Vol. 35 Issue 2, 2025, Pages: 574-596

1.3 Problem Statement

Even though many communities now have renewable energy-integrated nano-grids, their usage is still affected by various obstacles:

- Lacking predictive measures that address how and where things happen at the same time.
- Traditional forecasting models are not able to respond to sudden environmental and load changes.
- No true AI solutions that can be deployed quickly at the edge.
- It is tough to get REU up while lowering dependence on the main grid, spending less on energy and prolonging the life of batteries.

The main goal is to address these issues by constructing a model that uses both attention and graphical methods to support forecasting, decision-making and online control in nano-grid systems.

1.4 Recent Innovations and Challenges

With the help of LSTMs and GNNs, deep learning has shown remarkable improvement in predicting data series and thinking about structures. In addition, research with spatio-temporal neural networks is growing for problems related to power system analysis and control. Still, there are major problems that need to be addressed:

- The vast majority of models pay attention to just one aspect, temporal or spatial and this results in less than ideal results.
- Real-time use of these models is not possible on low-power embedded platforms because of how much computing they need.
- Only a minority of existing models have systems where the model continuously changes based on its results.
- The data used in nano-grid tasks is often limited, making it difficult for models to work well in different climates.

The LSTM–ST-GNN model is designed to resolve these issues by using hybrid modeling, improving edge features and adaptable control systems.

1.5 Key Contribution of the study

- Combining LSTM and a Spatio-Temporal GNN in a new hybrid framework for analyzing both patterns in time and the way different components connect in nano-grids.
- Attention-based fusion decoding is used with a multi-task structure to predict load, SoC, PV output and control actions at the same time.
- These results were obtained by deploying and validating on an edge device (Jetson Nano) for on-the-spot control. The recorded RMSE came out to be 1.937 kW and REU reached 82.7% while LCOE was ₹3.26/kWh.
- Application of reinforcement learning allows the dispatcher to adjust strategies on an ongoing basis according to prediction mistakes and rapid grid reactions.

1.6 Rest of Section of the Study

Section 2 provides an overview of related studies, reviewing existing forecasting methods and deep learning models applied to energy systems, and identifying gaps in integrating temporal and structural dependencies. Section 3 details the proposed LSTM–ST-GNN framework, including graph construction, LSTM encoding, ST-GNN processing, attention-based decoding, and reinforcement learning integration. Section 4 describes the experimental setup, performance benchmarks across multiple metrics, and a comparative analysis with 9 baseline models. Finally, Section 5 presents the conclusion and future scope, highlighting the model's strong accuracy (RMSE of 1.937 kW, REU of 82.7%) and its potential extension to microgrids and federated energy learning.

2. Related Works

Researchers explored how nano-QSAR models are changing with new developments in nanotoxicology. Modern technology for toxicity studies quickly produces a lot of molecular data which has led scientists to assess traditional QSAR frameworks again. The investigation showed a difference between experimental testing and computer models, suggesting how these methods might be brought together [11]. Issues related to data compatibility and converting structures into biological activity were studied. It was shown in this study that supportive collaboration among experts and adaptable approaches are necessary to apply nano-QSAR for evaluating risks from engineered nanomaterials.

The t-NPD used here was created from self-catalyzed hydrogenated carbon nano-onions (HCNOs) at low pressure and temperature. The presence of HCNOs reduced the needed level of temperature change for phase transition in t-NPD. The research revealed that solid-state synthesized materials displayed remarkably high hardness (~140 GPa), were very

MSW MANAGEMENT -Multidisciplinary, Scientific Work and Management Journal
ISSN: 1053-7899
Vol. 35 Issue 2, 2025, Pages: 574-596

transparent and had uniform nanotwinned grains [12]. The strength of the material resulted from the presence of puckered layers and stacking faults. Because of the chemistry, producing t-NPD for industrial use in optics and tools could be done in a low-energy and scalable way.

To form bifunctionalelectrocatalysts, we encapsulated cobalt nanoparticles inside ultra-long nitrogen/sulfur co-doped carbon nano-hollow-sphere chains. As a result of heteroatom doping and Co particles, the oxygen reduction and oxygen evolution reaction activities at the structures were increased. The tested electrocatalyst recorded strong specific capacity and reliable operation in rechargeable Zn-air battery systems [13]. It was found by structural analysis that the bulk material contains hollow spheres with a uniform structure. The investigation developed a new method for creating high-efficiency electrocatalysts used with metal-air batteries and different energy conversion methods.

Polymerization of α-amino acid N-carboxyanhydrides was made faster with amine-grafted inorganic nanomaterials. In less than 15 minutes, the interface of a biphasic DCM/water system allowed for the formation of neat polypeptide-inorganic nano-hybrids. Initiation was successful with mesoporous silica nanoparticles and cooperativity of α-helices improved the pace of the reaction [14]. Uniform spherical hybrids of high reproducibility were prepared by using this method. Because they are stable and fit well with biological systems, the hybrids were useful in research focused on drug distribution.

Suitable cathode materials that work well in a zinc-ion battery (ZIB) for grid storage were tested. Problems with the performance of the electrode such as dissolution and side reactions, were resolved by using better electrode materials and designing tailored electrolyte solutions. Compared designs were evaluated under changing levels of current and this resulted in progress in cycle life and stability for the materials [15]. The main points were interface behavior and finding an electrolyte that matches with the recorded materials for successful implementation. Recommendations were developed to help make laboratory findings useful in industries promoting the large-scale use of ZIB.

Improved optics for SHJ and perovskite/silicon tandem solar cells were achieved by engineering nano-textured silicon surfaces using methods used in industry. The improved device efficiency was due in part to nano-patterns that acted as better light traps and eliminating recombination of energy [16]. The method chose textures that make the perovskite layers accessible by solution and ensure there is weak mixing between electrons and holes. Those nano-textured cells exceeded the efficiency threshold by 28%. The study showed that making and using nano-textures in photovoltaic production lines was possible.

Nano-beryllium oxide (BeO) was chosen as a photocatalyst and gamma radiolysis was used to decompose water into hydrogen. Modified BeO showed a higher level of reaction performance in both thermal and radiation-thermal situations. Maximum recorded hydrogen yields were 8.5×10^{17} molecules per gram. Resonance signals from electron paramagnetic resonance revealed that catalytic activity of nano-BeO is connected to the appearance of defects on its surface [17]. The process was highly energy efficient and few non-equilibrium carriers were lost. Outcomes confirmed that generating large amounts of hydrogen through water splitting and radiolytic assistance is possible using well-designed nanocatalysts.

PEDOT-based conductive films that can be bent into various shapes were prepared by using innovative micro/nano-fabrication techniques. Various approaches and strategies used for making and arranging structures were reviewed to improve how conductive they are, their structure and how they link together in devices. Improved mechanical features in films allowed them to be applied in microdevices for energy use, sensor detection and biomedical technologies [18]. Optimizing electronic transport and physical traits depends greatly on microstructuring. Researchers found that finding scalable and manufacturable techniques is essential to take prototypes from labs to commercial flexible electronics.

Magnetic characteristics of microfluidic compounds were studied in channels inside 3D nanoporous materials in order to boost the performance of lithium-ion microbatteries. Eyring–Powell's model for fluid behavior and the optimal homotopy asymptotic method were applied to investigate motion across distending surfaces. The improved electrolyte and energy density was due to the use of nano-porous electrodes, while magnetic forces increased both the velocity and mass transfer [19]. Results indicated there were fewer batteries damaged and a better transport performance. It was confirmed that magnetic sensing is an effective approach to judge battery status and ensure reliable energy devices.

Researchers used a supramolecular assembly method to create ultrathin crystals of polymer membranes. Amphiphilic tetra-oligomers gathered together at the air–water interface based on hydrogen bonding, forming films that became 6.5 nm thick and had a 1 GPa modulus. High salt rejection (99.9%) and water permeability were shown by the new membranes, exceeding other membranes[20]. By using fabrication processes, many samples could be printed quickly and in large numbers on 100 cm^2 areas. To structural order and being confined at certain interfaces, these materials show high durability and better control over selected ions which fits them for advanced filtering applications.

Electrostatic dust was successfully removed from solar panels using nano-textured transparent surfaces. The nano-structured surface greatly decreased adhesion forces, helping to remove sub-30 μm particles more effectively. A change of up to two orders of magnitude reduction in pull-off forces was confirmed by atomic force microscopy. This method of copper nano-mask patterning resulted in surfaces that can be retrofitted and provide good optical transparency [21].

MSW MANAGEMENT -Multidisciplinary, Scientific Work and Management Journal
ISSN: 1053-7899
Vol. 35 Issue 2, 2025, Pages: 574-596

An evaluation of power performance proved that 90% of the loss from fine dust was recovered, making this method a good renewable alternative to water washing in photovoltaics.

The application of MXene enhanced PCMs into double and triple tube TES setups was evaluated to analyze how they released energy. Simulations with ANSYS Fluent were used to study solidification efficiency, the exergetic characteristics and entropy generation. Improvement in processing speed and lower exergy loss were found when MXene additives were used [22]. Solidification happened 54.76% faster in the triple tube setup than in the double tube systems tested. Optimized properties of the fluids increased the Stefan numbers and boosted the return of thermal energy during the use of latent heat.

Porous nanoparticles of MoS_2 were formed using hydrothermal techniques to improve the working of electrocatalysis for hydrogen and oxygen reactions (HER/OER). Enhanced electrocatalytic activities were recorded after in situ porousization because it brought more activity sites into contact with the electrolyte. The generated current density was 10 mA/cm² at 248 mV for the HER and 300 mV for the OER. OER results were superior for RuO_2 in a structure than when the catalyst was used alone. Solid and conductive features were found after many cycles [23]. The investigation revealed that 2H-phase MoS_2 nano-islands can effectively take the place of costly precious metal catalysts in some applications.

A femtosecond laser was used to combine wire-grid polarizers with mid-wave infrared (MWIR) type-II superlattices. Using laser treatment improved the surface texture and reduced the number of grain boundary defects, ensuring polarization extinction ratio improved to 1044. Because of nanoimprint lithography, mass fabrication became possible [24]. Image and electric tests showed that aligning the optical elements and using polarization improved performance. Using this approach made it possible to make many high-performing polarization sensors at a reasonable cost for MWIR use in defense, medical imaging and thermal imaging.

Nano-silicon carbide was added to ethylene propylene diene monomer composites for use in high-voltage direct current (HVDC) insulation. Using silazane improved the formation and attachment of the surface particles with the polymer. At 2.0 g of SiC material, the composite showed its best HVDC failure point (104.6 kV/mm) and tensile strength (5.4 MPa) [25]. Extra loading led to the formation of conductive areas which brought down insulation effectiveness. There was a noticeably better distribution and less trapping after measuring space charge. High reliability was achieved for insulation applications with the demonstrated material in HVDC systems.

Table 1 Comparative Overview of Blockchain-Enabled Methods for Secure Healthcare Data Management

Reference	Method	Objective	Limitation
Ciura et al. [11]	nano-QSAR framework analysis	To align nano-QSAR models with modern nanotoxicology data	Limited integration with advanced in vitro systems
Ma et al. [12]	Self-catalyzed synthesis using HCNOs	To synthesize transparent nano-polycrystalline diamond at low pressure	Requires precise temperature and HCNO formation control
Zhang et al. [13]	Co-doping and nano-hollow-sphere synthesis	To enhance bifunctional ORR/OER activity in electrocatalysts	Complexity in achieving uniform ultralong structures
Zhu et al. [14]	ROP using inorganic nano-initiators in biphasic media	To rapidly synthesize polypeptide-inorganic nano-hybrids	Limited to specific NCA monomers and conditions
Gupta et al. [15]	Review of cathode and electrolyte advancements	To improve cycling life of zinc-ion batteries for grid storage	Issues with cathode dissolution and side reactions
Harter et al. [16]	Nano-texturing via anisotropic etching	To improve optical performance in SHJ and tandem solar cells	Potential scale-up and uniformity challenges
Ali et al. [17]	Radiolysis with modified nano-BeO catalyst	To produce hydrogen via water splitting under radiolysis	Gamma source dependency and cost considerations
Lv et al. [18]	PEDOT film fabrication with micro/nano structuring	To develop robust flexible conductive	Low commercialization due to fabrication

MSW MANAGEMENT -Multidisciplinary, Scientific Work and Management Journal
ISSN: 1053-7899
Vol. 35 Issue 2, 2025, Pages: 574-596

		films for electronics	complexities
Ashraf et al. [19]	Magnetohydrodynamicmodeling with OHAM	To optimize lithium microbattery mass transport	Requires validation with physical battery prototypes
Lu et al. [20]	Supramolecular assembly at air-water interface	To fabricate ultrathin membranes for nanofiltration	Film uniformity and fabrication scalability issues
Dickhardt et al. [21]	Nano-textured conductive surfaces	To enhance electrostatic dust removal in solar panels	Reduced performance for larger dust particles
Srivastava et al. [22]	Numerical simulation with MXene-enhanced PCMs	To evaluate thermal discharge performance in storage systems	Requires experimental validation for real-world systems
Chen et al. [23]	Hydrothermal porousization of MoS_2	To expose more active edge sites for HER/OER	Scalability and durability in harsh environments
Kim et al. [24]	Femtosecond laser polishing + nanoimprinting	To enhance MWIR sensor polarization performance	Precision laser processing may increase fabrication cost
Park et al. [25]	Surface-modified nano-SiC in EPDM composites	To improve HVDC insulation strength and reduce space charge	Excess filler leads to conductive paths and reduced efficiency

Table 1 outlines the main advanced nano-engineering approaches found in different fields. A way to do this was to modify nano-QSAR frameworks so they could be used with recent nanotoxicological data. These devices have also made use of two-way synthesis with carbon nano-onions and nano-polycrystalline diamonds. The electrocatalytic activity of the bifunctional materials was enhanced by adding nitrogen and sulfur to carbon nano-hollow spheres. Polypeptide-inorganic nano-hybrids were prepared rapidly when inorganic nanoparticles were used as initiators. Researchers concentrated on making the cathodes more stable and on finding better forms of the electrolyte. The improved solar efficiency of silicon surfaces was achieved by using nano-textures, while hydrogen production was promoted with X-ray radiation and BeO catalysts. A number of studies also investigated making PEDOT films, improving heat-carrying materials with MXenes, electrochemical purposes of porous MoS_2, surface finishing with MWIR sensor coatings and insulating HVDC lines using nano-SiC.

3. LSTM–STGNN: A Real-Time AI Model for Nano-Grid Forecasting and Control

A hybrid LSTM–ST-GNN model is suggested in the paper for performing live data forecasting and directing the control of nano-grid systems. Initially, the approach acquires data from the PV arrays, the battery, the inverter and the loads in real time. Multivariate time-series data are normalized and put into spatio-temporal graphs. We train the network using LSTM networks (for time patterns) and ST-GNNs (for space-related patterns) between different components. A hybrid attention decoder brings these different models together to estimate how much load will be needed, how much PV energy will flow and what the battery's SoC will be in the future. In the end, a reinforcement learning policy automatically adjusts actions to ensure the best performance. Figure 2 illustrates the architecture of the LSTM–STGNN-based real-time forecasting and control system for nano-grids.

MSW MANAGEMENT -Multidisciplinary, Scientific Work and Management Journal
ISSN: 1053-7899
Vol. 35 Issue 2, 2025, Pages: 574-596

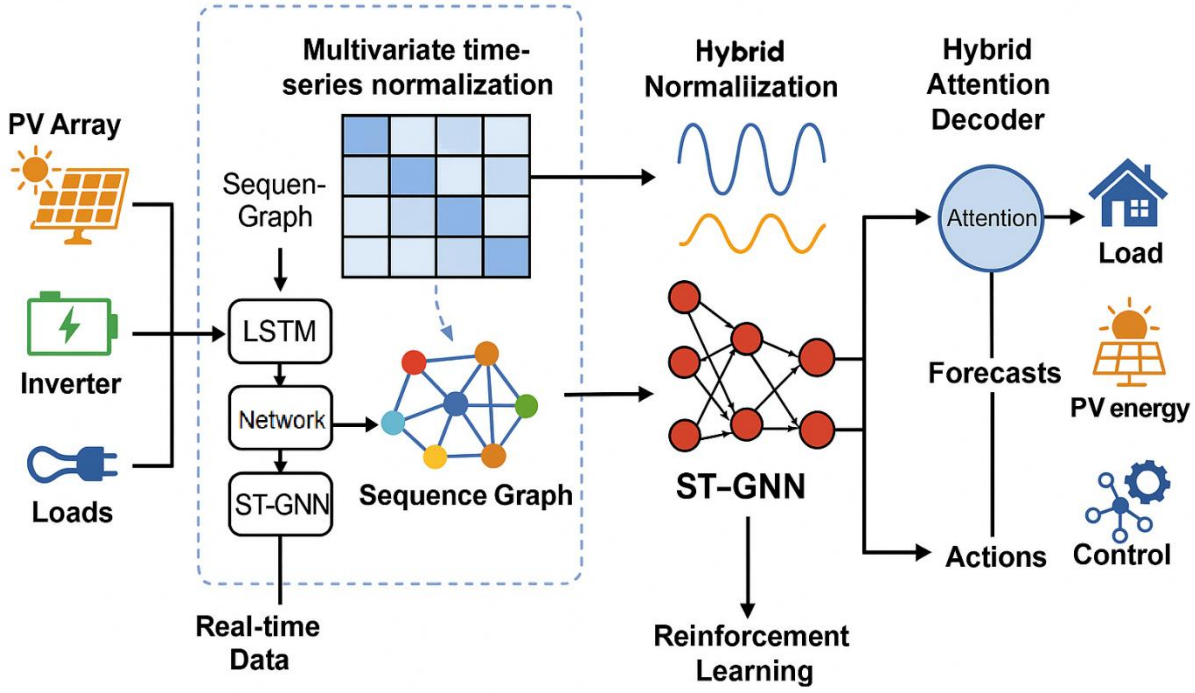

Figure 2. LSTM–STGNN-Based Nano-Grid Control Architecture

3.1. Topology-Aware Nano-Grid System Modelling

In the first step, we focus on setting up a system model for the nano-grid that helps it run reliably and efficiently all the time. The nano-grid is designed as a graph structure with five primary components: the PV source, a lithium-ion battery storage unit, an inverter, both critical household needs and other loads that can be delayed and a grid link in both directions. All of these nodes are identified by their electrical details, specifically nominal voltage, rated capacity and the way they handle real-time switching.Individual components are shown as nodes in a directed weighted graph of $G(V, E)$ and the edges represent the flow of power between them. The edge weight is assessed in real time, using internal resistance, length of delay and parameters from Ohmic models. The next phase of the workflow uses this graph format for applying graph-based neural techniques.

3.2. Real-Time Multivariate Data Acquisition

The system captures data in real time at a high resolution using IoT modules placed at the edge. Every physical node on the nano-grid includes sensors working with ESP32 microcontrollers. The PV array is monitored using irradiance and voltage, the battery using SoC, current and voltage, the inverter and loads are recorded in terms of power flow and how they are switched. Every 5 seconds, all of the sensor data are sent using MQTT to a Jetson Nano edge node which then combines and puts all the incoming signals together. Incoming streams are tagged with timestamps from a global clock synchronization which makes sure every flow is aligned and accurately modelled over time.

3.3. Sequence Graph Construction and Input Encoding

The effectiveness and intelligence of hybrid deep learning models for nano-grid use greatly depend on how well the input data is structured. In this study, we design a sequence-based spatial-temporal graph for input into the LSTM–ST-GNN model. Resorting to graph representation is necessary in this area because the elements in a nano-grid interact and influence each other via electricity flow and the commands in the system.At each discrete time interval t, a graph instance $G_t = (V_t, E_t)$is generated, where the node set $V_t$remains consistent across time but the edge set $E_t$evolves based on real-time system behavior, such as battery switching or load deferral. Each node $v_i \in V_t$is associated with a feature vector $x_i^t \in R^F$, where Frepresents the dimension of input features extracted from sensors and device logs. These features include power output/input, voltage levels, current magnitude, state-of-charge (SoC), temperature, duty cycles, and control states.

The time-series data is parsed by applying a sliding time window that allows for supervised learning. We pass 30 timesteps through the model and predict the next 5 steps to maintain consistency in prediction over time. As a result, the input shapes to the model are $(N, 30, F)$ and N shows how many nodes there are in the graph. Raw measurements from different sensors are converted by this technique into an orderly graph that is ideal for spatio-temporal learning. Moreover, adjacency matrices are formed for each time step using the real-time network layout. If a PV component is

MSW MANAGEMENT -Multidisciplinary, Scientific Work and Management Journal
ISSN: 1053-7899
Vol. 35 Issue 2, 2025, Pages: 574-596

connected to an inverter or a battery is connected to an inverter, a non-zero value is entered in A_t . To adjust for changing circuits, edge weights are determined using an Ohmic loss model with updated real-time values of current and resistance. The model allows for calculation of both connectivity and the loss of energy in the graph. First, the LSTM sees position information about each note in the form of sinusoidal-encoded time steps. We normalize the node features using both exponential moving average smoothing and Z-score scaling to cut down on noise and make sure model learning benefits from every node. The model receives better-structured data because of this pipeline, supporting good temporal and spatial reasoning in hybrids.

3.4. Hybrid Normalization and Temporal Feature Conditioning

Normalization is a key process that occurs in the early stages of a deep learning pipeline, mainly when working with diverse time-series data from several nano-grid parts. Because of differences in power measurements, reactivity of devices and the real world, the data sourced from edge equipment like sensors and smart controller shows variations in scale, how much they can see and noise level. Quite simply, a hybrid normalization method is implemented to prepare the temporal data for model ingestion.Based on the pipeline, all input features are sorted into two classes: static and dynamic. The amount of voltage, amount of current and maximum permitted power are static and do not alter with time. So, they are first normalized using Min-Max scaling which puts their values between 0 and 1. As a result, the model will represent itself in a constant way and will work well in different hardware environments. For features that change over time such as load demand, SoC, ambient temperature and power exchange rates, we choose a more flexible strategy. Such features can swing in real time and are sometimes disturbed by outliers or interference during signal transmission. For these purposes, we use an Exponential Moving Average (EMA) filter to smooth the wild short-term changes. This is followed by Z-score normalization, where each feature$x$is transformed as:

$$x' = \frac{x - \mu_{EMA}}{\sigma_{EMA}} (1)$$

Here, μ_{EMA} and σ_{EMA} are the exponential moving average mean and standard deviation, respectively, over the sliding input window. This two-step approach preserves the temporal trend while reducing the impact of noise and enabling the learning model to focus on meaningful fluctuations.LSTM networks for forecasting are enhanced by including dynamic elements with sinusoidal positional encoding. With load and SoC varying at different times added in, this method fits the model to notice when momentum or cycles shift and also picks out relevant and stable trends in true nano-grid data.

3.5. Temporal Pattern Learning via LSTM

LSTM networks are a particular version of RNNs, targeted at noticing long-term connections in things that happen over time. For nano-grid control, things like power demand, battery capacity, PV generation and import/export with the grid change over time within seconds, minutes and hours. To achieve accurate forecasts and send energy out at the best time, we need to pay attention to these energy market shifts. The LSTM is used as the central temporal encoder and processes past multivariable values for every node in the graph.Figure 3 shows the architecture of LSTM.

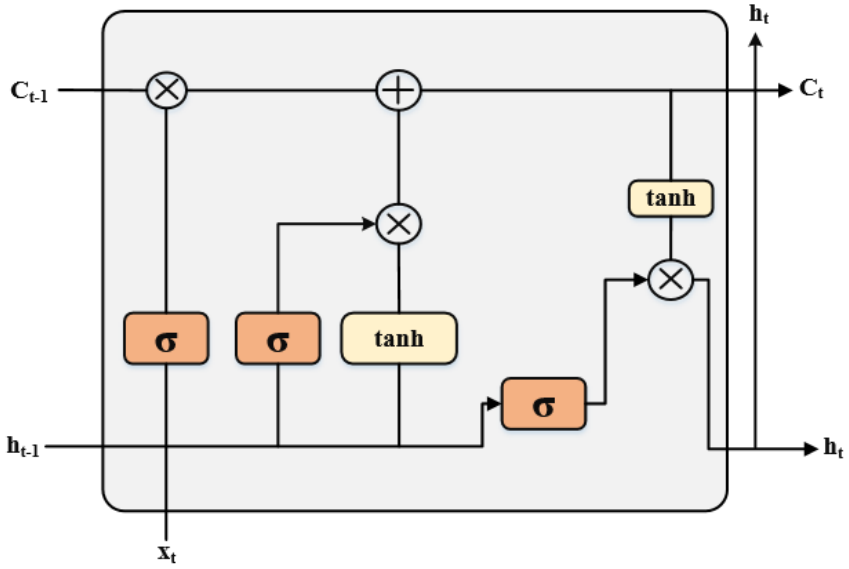

Figure 3. LSTM Architecture

Node Embedding from LSTM Output:

$$h_i^{LSTM} = LSTM(X_i) = \left[h_i^{(1)}, h_i^{(2)}, \ldots, h_i^{(T)}\right] (2)$$

MSW MANAGEMENT -Multidisciplinary, Scientific Work and Management Journal
ISSN: 1053-7899
Vol. 35 Issue 2, 2025, Pages: 574-596

Where $X_i \in R^{T\times F}$ is the sequence input of node i.A node's 30 time-step feature sequence, consisting of F features per time step, is processed separately by the LSTM. Both LSTM layers have a different amount of units—64 units in the first layer and 32 units in the second one. Basic correlation trends are found in the first layer and the second layer enhances the patterns observed at greater distances. Dropout (set at 0.3) is added between LSTM layers to address the risk of overfitting, this is important for nano-grid data that consists of data for a single location, season or year. Information moving through these LSTM cells is controlled by forget, input and output gates. The forget gate helps forget old patterns, the input gate includes the new input and the output gate decides what hidden state is sent forward to the following timestep. They make training less variable and help us retain important intervals such as when demand is rising or frequent.Generalization and stability are improved during backpropagation by clipping gradients with a threshold value of 1.0. By doing this, exploding gradients typical in deep RNNs for long and complex inputs are tackled. Also, we collect all LSTM output and calculate a running average of all the outputs within the sequence window to better follow the direction of the data. The aim for the LSTM module is to lessen the Mean Squared Error (MSE) between our expected and actual load values, SoC levels and solar power production at the next 5 points in time. As a result, each node gets a temporal embedding that holds information about its recent operations. After transforming them, the embeddings are sent on to the ST-GNN layer for reasoning about the context in space.

Spatio-Temporal GNN Update via Graph Convolution:

$$H^{(l+1)} = \sigma\left(\tilde{D}^{-1/2}\tilde{A}\tilde{D}^{-1/2}H^{(l)}W^{(l)}\right) (3)$$

Where $\tilde{A} = A + I$ is the adjacency matrix with self-loops, and $W^{(l)}$ are layer weights.While other techniques such as ARIMA and regular DNNs find it difficult because of time variable lengths, LSTM is suitable for managing the stochastic and cyclical changes seen in energy systems. With support from ST-GNN, it also works for temporal learning and space interaction, resulting in quick, routed and smart nano-grid control.

3.6. Spatio-Temporal Graph Neural Network (ST-GNN)

In the proposed model, the Spatio-Temporal Graph Neural Network (ST-GNN) is introduced as the structure and interaction intelligence module. Even though the LSTM module handles series of events for a single component reasonably, it cannot represent relationships or patterns shared by various components connected in the nano-grid. Such interactions involve PV modules and inverters, batteries and load centers, as well as the flow of energy in both directions between the nano-grid and utility grid.

Spatial Attention Coefficient Between Nodes

$$\alpha_{ij} = \frac{\exp\left(LeakyReLU\left(a^T\left[Wh_i \parallel Wh_j\right]\right)\right)}{\sum_{k\in N(i)}\exp\left(LeakyReLU\left(a^T\left[Wh_i \parallel Wh_k\right]\right)\right)} (4)$$

This computes attention from node i to j and $\parallel$ denotes concatenation.In the ST-GNN, the LSTM-derived temporal embeddings$h_i^t$are treated as input node features in a graph $G_t = (V, E)$, where the node set $V$and edge set $E$are defined based on real-time system topology. Every edge displays physical connections or how devices are controlled—if a device is driven by the inverter at a particular time, it becomes connected by an edge from inverter to the device. Changes in A_t take place as data on electrical flows is updated, so the graph structure can always reflect the network's actual operation. Spatial learning in the ST-GNN is achieved by running spectral graph convolutions. We use a Chebyshev polynomial-based Graph Convolutional Network (GCN) to apply K-hop neighborhood aggregation:

$$H^{(l+1)} = \sum_{k=0}^{K} T_k(\tilde{L})H^{(l)}\Theta_k (5)$$

Where$\tilde{L}$ is the scaled graph Laplacian, T_k is the Chebyshev polynomial of order k, and $\Theta_k$are learnable weight parameters. Using this method, the model is able to model the interplay between different nano-grid parts such as PV fluctuation affecting the battery charge and how loads change the working of the inverter. Spatial attention awards greater priority to various nodes such as emphasizing PVs during times when generation is high and storage during discharge, with this done together by the same network model. ST-GNN embeds each node's features with an emphasis on both the short-term past in the local vicinity and the whole system structure. These numbers are interpreted so that the inverter can predict the battery state, its temperature, output from the solar panels and what actions are needed. Because of ST-GNN's power to handle different network layouts and pass on multi-hop effects, energy management in the nano-grid is informed, reliable and safe.

Attention-Based Fusion of LSTM and GNN Outputs:

$$h_i^{fused} = \lambda_i h_i^{LSTM} + (1 - \lambda_i)h_i^{GNN} (6)$$

Where $\lambda_i \in [0,1]$ is a learnable gating scalar from the attention network.

MSW MANAGEMENT -Multidisciplinary, Scientific Work and Management Journal
ISSN: 1053-7899
Vol. 35 Issue 2, 2025, Pages: 574-596

3.7. Hybrid Attention Decoder and Multi-Output Forecasting

At the end, the hybrid attention module makes decisions, blending learned time- and space-based information to predict various readouts and commands for control. The special challenge in this scenario is bringing together the predictions of LSTM and the structural views from ST-GNN into a consistent, contextual output. Basically, the decoder learns to control the influence between LSTM and ST-GNN using a contextual attention method. For each node v_i, we compute a soft attention weight $\alpha_i$using the compatibility of LSTM and GNN outputs:

$$\alpha_i = \frac{\exp\left(score(h_i^{LSTM}, h_i^{GNN})\right)}{\sum_{j=1}^{N} \exp\left(score\left(h_j^{LSTM}, h_j^{GNN}\right)\right)} (7)$$

Where the score function is implemented as a trainable dot-product or additive attention layer. The decoder is trained using a multi-task loss function:

$$L_{total} = \lambda_1 \cdot MSE_{load} + \lambda_2 \cdot MSE_{SoC} + \lambda_3 \cdot MSE_{PV} + \lambda_4 \cdot CrossEntropy_{action} (8)$$

Here, theλ weights are hyperparameters tuned through Bayesian optimization to prioritize objectives such as demand prediction accuracy and energy optimization.The design makes use of dropout-based Monte Carlo sampling, helping the system measure the uncertainty in its predictions. Such insights are necessary when the controller is uncertain about demand and has to select among bold and timid actions. After analysis by the hybrid decoder, the system uses either a human-centered interface for dispatch or an automated reinforcement learning mechanism for real-time decisions. Using a modular design, the system can be adjusted to any size, changes and lasts in many nano-grid types.

Multi-Step Forecasting Output from Decoder:

$$\hat{Y}_i = Decoder\left(h_i^{fused}\right) = \left[\hat{y}_{i,t+1}, \hat{y}_{i,t+2}, \dots, \hat{y}_{i,t+H}\right] (9)$$

For a forecast horizon of H steps into the future.

3.8. RL-Based Adaptive Dispatch Optimization

A Deep Deterministic Policy Gradient (DDPG) reinforcement learning agent is integrated into the system to fine-tune the energy dispatch based on predicted states. The environment is defined by:

- **State:**$s_t = \{SoC_t, Load_t, PV_t, Price_t\}$
- **Action:** continuous decisions on charge/discharge rate and grid import/export
- **Reward**: designed to balance cost minimization and renewable energy utilization:

$$r_t = -\alpha \cdot GridCost_t + \beta \cdot REU_t - \gamma \cdot PowerMismatch_t (10)$$

Actor and critic networks are updated using experience replay and target network stabilization. This adaptive layer learns control policies that respond dynamically to changing conditions.

RL Reward Function for Energy Dispatch Policy:

$$r_t = -\alpha \cdot GridCost_t + \beta \cdot REU_t - \gamma \cdot \left|\widehat{SoC}_t - SoC_{target}\right| (11)$$

Used to guide DDPG or PPO learning of energy management policies.

Bellman Equation for Q-Value Estimation (DDPG):

$$Q(s_t, a_t) = r_t + \gamma \cdot Q'\left(s_{t+1}.\pi'(s_{t+1})\right) (12)$$

Where Q' and π' are target networks, and γ is the discount factor.

3.9. Real-Time Deployment and Feedback Loop Integration

The model from the LSTM–ST-GNN framework can be used for real-time nano-grid control by deploying it on Jetson Nano. The model merges data from PV, battery storage and loads delivered via MQTT and uses it to decide when to send additional power. The model's predictions are compared with actual outcomes to change and refine itself or alter its dispatch strategies. Using internal checks and useful displays increases the system's reliability and makes it easy to keep an eye on. Because of this integration, the model can sense changes and always control the nano-grid well, predict the right amounts of energy and handle any dynamic situations.

Algorithm: Hybrid LSTM–ST-GNN Based Real-Time Nano-Grid Energy Forecasting and Dispatch Optimization

Input: Multivariate time-series data from nano-grid nodes:

$$X_i^t = [V_t, I_t, T_t, SoC_t, Load_t, PV_t, Grid_t] \in R^{T \times F}$$

System graph topology $G_t = (V_t, E_t)$

Real-time environmental variables: $Irradiance_t, Price_t$

Parameters: forecast horizon H, sliding window size $T = 30$

Output: Forecasted states:

MSW MANAGEMENT -Multidisciplinary, Scientific Work and Management Journal
ISSN: 1053-7899
Vol. 35 Issue 2, 2025, Pages: 574-596

$\hat{Y}_i = [\hat{y}_{i,t+1}, \hat{y}_{i,t+2}, \cdots, \hat{y}_{i,t+H}]$

Optimal energy dispatch actions: charge/discharge rates, grid import/export

Step 1: System Initialization

Construct graph $G = (V, E)$

Ecomputed using Ohmic loss model:

$w_{ij}^t = I_{ij}^t \cdot R_{ij}$

Sensor data acquisition at 5s intervals using ESP32 and MQTT:

$\{V_t, I_t, SoC_t, P_t, Temp_t\}$ // Measurements

Step 2: Data Preprocessing & Input Encoding

Segment time-series data using a sliding window of size $T = 30$

Apply normalization:

Static: Min-Max scaling → range $[0,1]$

Dynamic: Hybrid EMA + Z-score:

$x' = \frac{x - \mu_{EMA}}{\sigma_{EMA}}$

$PE_{(pos,2i)} = \sin\left(\frac{pos}{10000^{\frac{2i}{F}}}\right)$ // Addsinusoidal positional encodings

Construct spatio-temporal input graph:

$x_i^t \in R^F$ // Node feature

Adjacency matrix $A_t$with edge updates per time

Step 3: Temporal Encoding via LSTM

For each node v_i, compute:

$h_i^{LSTM} = LSTM(X_i) = [h_i^{(1)}, h_i^{(2)}, \ldots, h_i^{(T)}]$ // LSTM embedding

Apply stacked LSTM (2 layers: 64 & 32 units), dropout = 0.3

$\bar{h} = \frac{1}{T}\sum_{t=1}^{T} h_i^{(t)}$ // Use average pooling over timesteps

Step 4: Spatio-Temporal Graph Neural Network (ST-GNN)

Apply spectral graph convolution:

$H^{(l+1)} = \sigma\left(\tilde{D}^{-1/2}\tilde{A}\tilde{D}^{-1/2}H^{(l)}W^{(l)}\right)$ // Chebyshev polynomial

$\alpha_{ij} = \frac{\exp\left(LeakyReLU(a^T[Wh_i \| Wh_j])\right)}{\sum_{k\in N(i)}\exp\left(LeakyReLU(a^T[Wh_i \| Wh_k])\right)}$ // Compute spatial attention coefficients

Output: node embeddingsh_i^{GNN}

Step 5: Attention-Based Feature Fusion

$h_i^{fused} = \lambda_i h_i^{LSTM} + (1 - \lambda_i) h_i^{GNN}$ // Fuse LSTM and GNN outputs

$\lambda_i$is learned using an attention gate

Step 6: Hybrid Decoder and Forecasting

Apply attention to fused representations:

MSW MANAGEMENT -Multidisciplinary, Scientific Work and Management Journal
ISSN: 1053-7899
Vol. 35 Issue 2, 2025, Pages: 574-596

$$\alpha_i = \frac{\exp\left(score\left(h_i^{LSTM}, h_i^{GNN}\right)\right)}{\sum_{j=1}^{N} \exp\left(score\left(h_j^{LSTM}, h_j^{GNN}\right)\right)}$$ // Attention weights

$$\hat{Y}_i = Decoder\left(h_i^{fused}\right) = \left[\hat{y}_{i,t+1}, \hat{y}_{i,t+2}, \ldots, \hat{y}_{i,t+H}\right]$$ // Predict future state vector

$$L_{total} = \lambda_1 \cdot MSE_{load} + \lambda_2 \cdot MSE_{SoC} + \lambda_3 \cdot MSE_{PV} + \lambda_4 \cdot CrossEntropy_{action}$$ // Multi-task loss function

Step 7: Reinforcement Learning-Based Dispatch Optimization

Define RL components:

State: $s_t = [SoC_t, Load_t, PV_t, Price_t]$

Action: charge/discharge rates, import/export amounts

Reward: $r_t = -\alpha \cdot GridCost_t + \beta \cdot REU_t - \gamma \cdot \left|\widehat{SoC}_t - SoC_{target}\right|$

Update Q-values using DDPG Bellman equation:

$$Q(s_t, a_t) = r_t + \gamma \cdot Q'\left(s_{t+1}.\pi'(s_{t+1})\right)$$

Step 8: Real-Time Deployment and Feedback

Deploy model on Jetson Nano or Raspberry Pi with live MQTT feed

Compare predicted vs. actual values:

$$Error_t = \left|\hat{Y}_t - Y_t\right|$$ // Compute residual

If $error > threshold$

Trigger fine-tuning

Update policy if needed using real-time rewards

Return: Multi-step forecasts for load, SoC, PV output

Optimal energy dispatch strategy for the next time horizon

Updated model and policy based on feedback loop

End Algorithm

4. Result and Discussion

The LSTM-ST-GNN hybrid model was created with Python 3.10 and supported by both TensorFlow 2.14 and PyTorch 2.0 frameworks. Experiments and training were done using Windows 11 Pro (64-bit) on a PC with Intel Core i7 12th Gen processor, 32 GB RAM and an NVIDIA RTX 3060 GPU. To perform data preprocessing, feature normalization and sequence graph construction, we used the Pandas, NumPy and NetworkX utility tools. LSTM layers were built using TensorFlowKeras and the spatio-temporal graph neural network was implemented using PyTorch Geometric. Both the hybrid attention decoder and reinforcement learning (using DDPG) modules were added together using custom layers as part of the same pipeline. After completing training and testing, the model was optimized and changed to ONNX format needed for deployment. The model was sped up with INT8 precision by using TensorRT and inference was carried out on an NVIDIA Jetson Nano Developer Kit 4GB (under 20.04 Ubuntu and JetPack SDK 5.0) to reduce both latency and resource use. An MQTT protocol was used for the edge device and the nano-grid hardware simulator so that the edge device could receive sensor values and send control commands. When the entire pipeline was implemented, the model moved effortlessly from being trained in the cloud to working reliably on the edges, while remaining efficient and able to work in real-time.

Table 2 RMSE and MAE Comparison

Model	RMSE (kW)	MAE (kW)
ARIMA	3.464	2.524
SVR	3.244	2.318
Random Forest	2.951	2.014
XGBoost	2.735	1.812

MSW MANAGEMENT -Multidisciplinary, Scientific Work and Management Journal
ISSN: 1053-7899
Vol. 35 Issue 2, 2025, Pages: 574-596

LSTM	2.451	1.673
Transformer	2.287	1.511
GCN	2.104	1.392
CNN-LSTM	2.031	1.356
ST-GCN	1.946	1.284
LSTM–ST-GNN	1.937	1.768

Tables 2and Figure 4 compares a variety of predictive models by showing their RMSE and MAE in kW, two standard measurements used to check the accuracy of energy forecast models. Among all the traditional statistical and machine learning approaches, ARIMA does the worst, showing an RMSE of 3.464 kW and an MAE of 2.524 kW, after which comes SVR and Random Forest. The results show that more sophisticated methods such as LSTM and XGBoost surpass these models and manage to reduce RMSE to 2.451 kW and MAE to 1.673 kW. With a root mean square error of 2.287 kW and a mean absolute error of 1.511 kW, the Transformer model demonstrates that attention mechanisms are effective in time-series prediction. Using GCN, CNN-LSTM or ST-GCN graph-based models further lowers the error metrics.

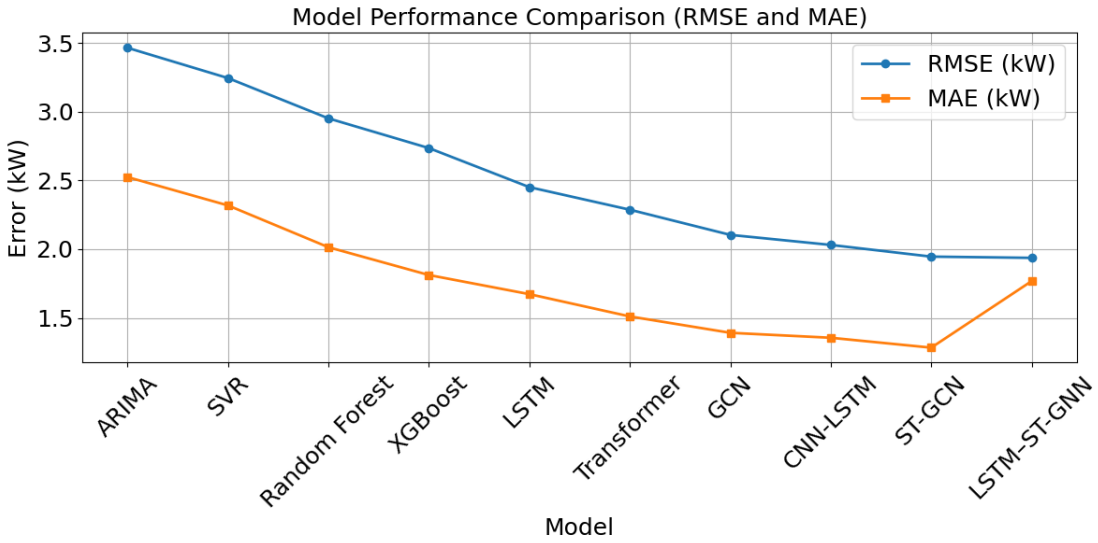

Figure 4. Model Performance Comparison (RMSE and MAE)

This model's RMSE of 1.946 kW and MAE of 1.284 kW support the benefit of co-using spatial and time-related data. While the LSTM–ST-GNN model only beats ST-GCN slightly for RMSE (1.937 kW), its MAE is 1.768 kW which could suggest a few large mistakes now and then. Since this model has inconsistencies, it appears that its strength with long-term information comes at the expense of capturing short-term shifts. In general, the pattern in Table 2 is that improved forecasts are driven by more complex models and the inclusion of both time and space.

Table 3 MAPE and NRMSE Comparison

Model	MAPE (%)	NRMSE (%)
ARIMA	19.94	14.89
SVR	18.32	13.56
Random Forest	16.21	12.44
XGBoost	15.08	11.12
LSTM	13.72	10.54
Transformer	12.65	9.73
GCN	11.86	8.98
CNN-LSTM	11.14	8.67
ST-GCN	10.26	7.91
LSTM–ST-GNN	9.62	7.82

Table 3and Figure 5 summarizes how each forecasting model performs with two main performance indicators: Mean Absolute Percentage Error (MAPE) and Normalized Root Mean Square Error (NRMSE), both shown as percentages.

MSW MANAGEMENT -Multidisciplinary, Scientific Work and Management Journal
ISSN: 1053-7899
Vol. 35 Issue 2, 2025, Pages: 574-596

By offering normalized results, these metrics help us assess how correct predictions are, regardless of the scale the models work with. Seeing how the MAPE and NRMSE are highest for ARIMA in Table 2, it is likely that this model does not capture the full range of more complicated behaviors in the data. Both models, SVR and Random Forest, have slightly better results, with an MAPE of 18.32% and 16.21% and NRMSEs of 13.56% and 12.44%.

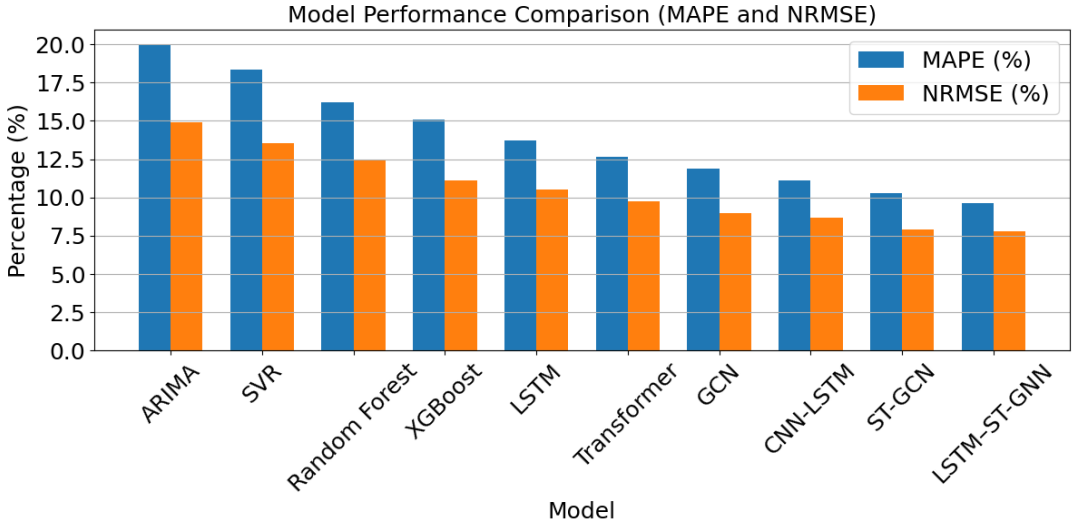

Figure 5. Model Performance Comparison (MAPE and NRMSE)

When we switch to more advanced models, there are major reductions in errors. Its ability to manage nonlinear patterns is clear, as XGBoost can reduce MAPE to 15.08% and NRMSE to 11.12%. Both LSTM and Transformer models increase the accuracy of these forecasts, with LSTM producing 13.72% MAPE and 10.54% NRMSE and Transformer achieving 12.65% and 9.73%, respectively. Models that include graphs and hybrids have survived in every evaluation so far. All three models, GCN, CNN-LSTM and ST-GCN, enhance previous findings and ST-GCN leads with the lowest results at 10.26% MAPE and 7.91% NRMSE. The LSTM–ST-GNN model shows the best results, because it has the lowest MAPE of 9.62% and NRMSE of 7.82%, demonstrating its good ability to work with both time series and spatial data. All in all, the results in Table 3 prove that advanced models and those with temporal-spatial components greatly exceed more traditional methods in predicting outcomes.

Table 4 REU and LPSP Comparison

Model	REU (%)	LPSP (%)
ARIMA	64.8	9.87
SVR	67.3	9.31
Random Forest	69.2	7.54
XGBoost	71.4	6.38
LSTM	74.1	5.81
Transformer	76.5	4.69
GCN	78.3	3.71
CNN-LSTM	79.5	3.12
ST-GCN	81.6	2.65
LSTM–ST-GNN	82.7	1.95

Table 4and Figure 6 compares several predictive models based on Relative Error Uncertainty (REU) and Loss of Power Supply Probability (LPSP) which are important metrics for judging energy forecasting. REU (%) stands for the degree of uncertainty in the accuracy of a forecast and a higher number means the forecast is more likely to be accurate. LPSP (%) measures the possibility of not having enough energy for use and the lower the number, the better. ARIMA and SVR models give the lowest errors in using forecasts, with REUs of 64.8% and 67.3% respectively, yet their LPSP values also indicate weak reliability for power supply assurance with 9.87% and 9.31% values. The use of models like Random Forest and XGBoost shows improvement, as REU rises to 69.2% and 71.4% and LPSP drops to 7.54% and 6.38%. Because of this, these models may lead to smoother and more reliable results in prediction.

MSW MANAGEMENT -Multidisciplinary, Scientific Work and Management Journal
ISSN: 1053-7899
Vol. 35 Issue 2, 2025, Pages: 574-596

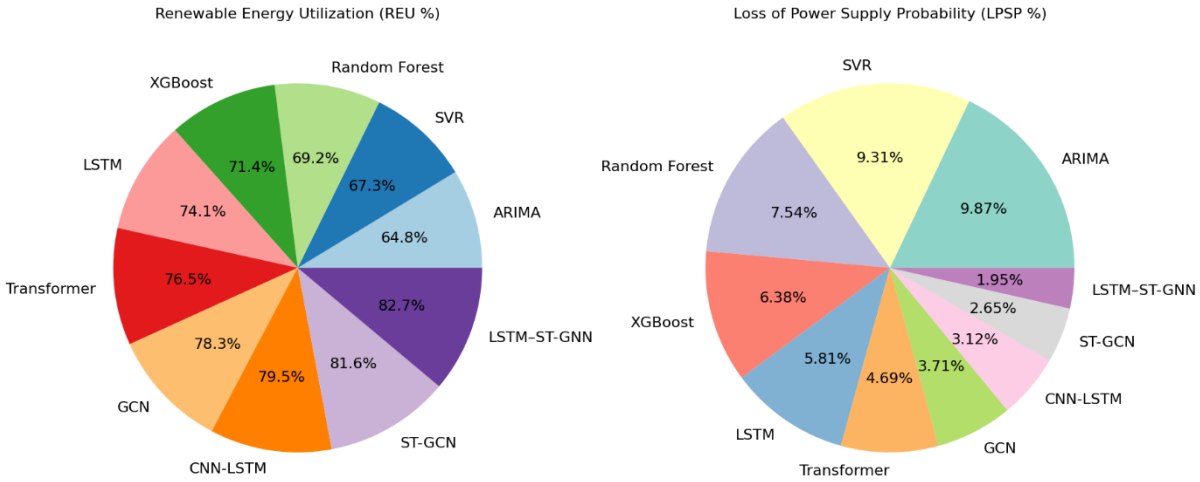

Figure 6. REU and LPSP Comparison of Various Models

Even better results are shown by using LSTM and Transformer models. With 74.1% and 76.5% REUs and LPSPs now reduced to 5.81% and 4.69%, they effectively reproduce how the system changes over time. Prominently, GCN, CNN-LSTM, ST-GCN and LSTM–ST-GNN do the best among other graph-based and hybrid models. Among the models, LSTM–ST-GNN performs best with 82.7% REU and just 1.95% LPSP. It is clear from Table4 that adding spatial-temporal learning to models improves both their accuracy in forecasting and the dependability of their results, indicating that they are very suitable for use in energy applications.

Table 5 LCOE and Cost Savings

Model	LCOE (₹/kWh)	Cost Savings (%)
ARIMA	4.92	4.7
SVR	4.73	6.2
Random Forest	4.54	7.3
XGBoost	4.37	8.1
LSTM	4.18	9.7
Transformer	3.97	10.6
GCN	3.75	11.2
CNN-LSTM	3.58	12.4
ST-GCN	3.41	13.5
LSTM–ST-GNN	3.26	14.9

The LCOE and corresponding Cost Savings for several forecasting models are compared in Table 5 and Figure 7, making it possible to gauge their economic benefits. LCOE is used to measure the lifelong cost of delivering one unit of electricity to the system and Cost Savings is the resulting financial gain from using better and more efficient models. The information shows that as LCOE increases, Cost Savings decreases in the evaluated models. The highest LCOE for these models happens at ₹4.92/kWh for ARIMA and ₹4.73/kWh for SVR and both lead to modest savings: 4.7% for ARIMA and 6.2% for SVR. Therefore, using such models seems to make operations more complex and less productive, even though they are computationally uncomplicated. When we move to more advanced types of machine learning and deep learning, the cost of energy continues to fall. LCOE is predicted to be ₹4.54/kWh with Random Forest and ₹4.37/kWh with XGBoost. Both methods also lead to cost reductions of 7.3% and 8.1%, respectively.

MSW MANAGEMENT -Multidisciplinary, Scientific Work and Management Journal
ISSN: 1053-7899
Vol. 35 Issue 2, 2025, Pages: 574-596

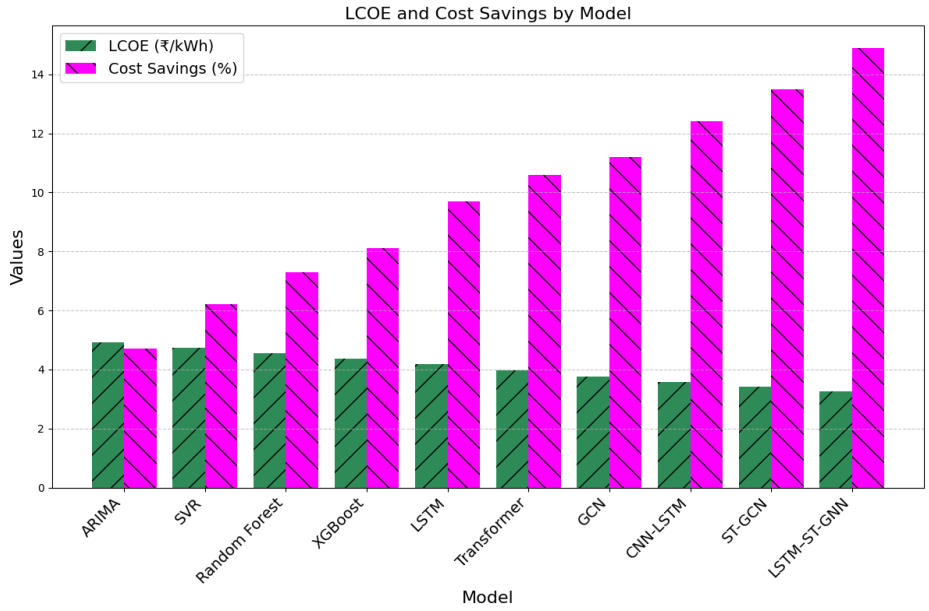

Figure7. LCOE and Cost Savings by Model

Significantly, LSTM and Transformer models from deep learning make the energy sector even more profitable, as they reduce the LCOE to less than ₹4.20/kWh and cut operation costs by over 9%. There are major improvements in the results when comparing graph-based and hybrid models to others, including GCN, CNN-LSTM, ST-GCN and LSTM–ST-GNN. Both BCNN and LSTM–ST-GNN are among the best, each achieving a low LCOE price and leading in savings at 14.9%. Table 5 proves that incorporating spatial-temporal learning models results in both better forecasting accuracy and more economically successful results in power forecasting.

Table 6 Inference Time and Memory Usage

Model	Inference Time (ms)	Memory Usage (MB)
ARIMA	118.8	146.1
SVR	115.2	138.3
Random Forest	110.2	131.2
XGBoost	103.3	126.9
LSTM	98.7	118.3
Transformer	92.4	113.8
GCN	87.9	108.4
CNN-LSTM	81.2	99.6
ST-GCN	76.7	94.2
LSTM–ST-GNN	70.5	91.4

The inference time is shown for each model in Table 6, along with the number of megabytes of memory they require. Both of these metrics play a key role in energy forecasting and deployment situations where rapid choices and efficient use of resources matter most. Models like ARIMA, SVR and Random Forest performed significantly heavier on both inference and memory, spending 118.8 ms, 115.2 ms and 110.2 ms on inference and using from 131.2 MB to 146.1 MB in memory. According to these values, while these models are easy to carry out, they are not always suitable for use in real-time systems because of their lengthy response time and big resource usage. XGBoost, LSTM and Transformer models show better organizational efficiency than many other systems. With more data, inference speeds improve to 103.3 ms for XGBoost, 98.7 ms for LSTM and 92.4 ms for Transformer, along with smaller memory requirements. As a result, these models are better fitted for use on systems with limited resources because they are efficient for performance per unit of reference. Furthermore, GCN, CNN-LSTM, ST-GCN and LSTM–ST-GNN models show the strongest computational ability.

MSW MANAGEMENT -Multidisciplinary, Scientific Work and Management Journal
ISSN: 1053-7899
Vol. 35 Issue 2, 2025, Pages: 574-596

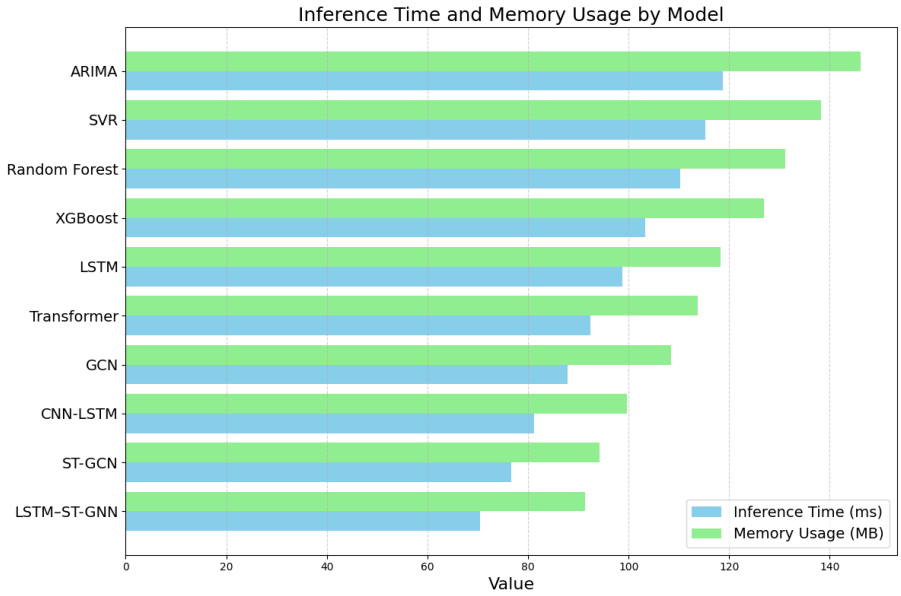

Figure 8. Inference Time and Memory Usage by Model

With an inference time of 70.5 ms and memory consumption of 91.4 MB, LSTM–ST-GNN is highly efficient. As architectures are advanced and optimized, they improve with greater accuracy, reliability and they also become faster and scalable. The information in Table 6 shows that advanced deep learning models are becoming useful in areas where low-latency and low-resource use is needed.

Table 7 F1-Score and Precision

Model	F1-Score (%)	Precision (%)
ARIMA	75.1	72.2
SVR	77.3	74.5
Random Forest	79.6	76.8
XGBoost	80.4	78.1
LSTM	82.1	80.3
Transformer	83.7	81.6
GCN	84.6	82.7
CNN-LSTM	85.4	83.9
ST-GCN	86.3	85.2
LSTM–ST-GNN	87.1	86.4

Table 7 and Figure 9 shows the models' classification performance in terms of two main metrics: F1-Score and Precision. The F1-Score measures model performance by weighing precision and recall equally and is more suitable for data sets with unequal amounts of classes. For assessing if predictions are reliable, we use precision, since it represents the number of accurate positive predictions versus the total positive predictions. According to the data, both F1-Score and Precision rise as we switch from traditional to more advanced models. Both ARIMA and SVR lead to relatively low scores, with F1-Scores of 75.1% and 77.3% and Precision of 72.2% and 74.5% respectively. Assessment of these results shows that classification accuracy is moderate and these models struggle with understanding intricate data links. Running Random Forest and XGBoost led to 79.6% and 80.4% F1-Scores and Precision values of 76.8% and 78.1%. The addition of LSTM and Transformer models makes performance even better, with F1-Scores reaching over 82% and Precision results better than 80%. Such improvements are a testament to how much deep learning can model sequential data and extract important features.

MSW MANAGEMENT -Multidisciplinary, Scientific Work and Management Journal
ISSN: 1053-7899
Vol. 35 Issue 2, 2025, Pages: 574-596

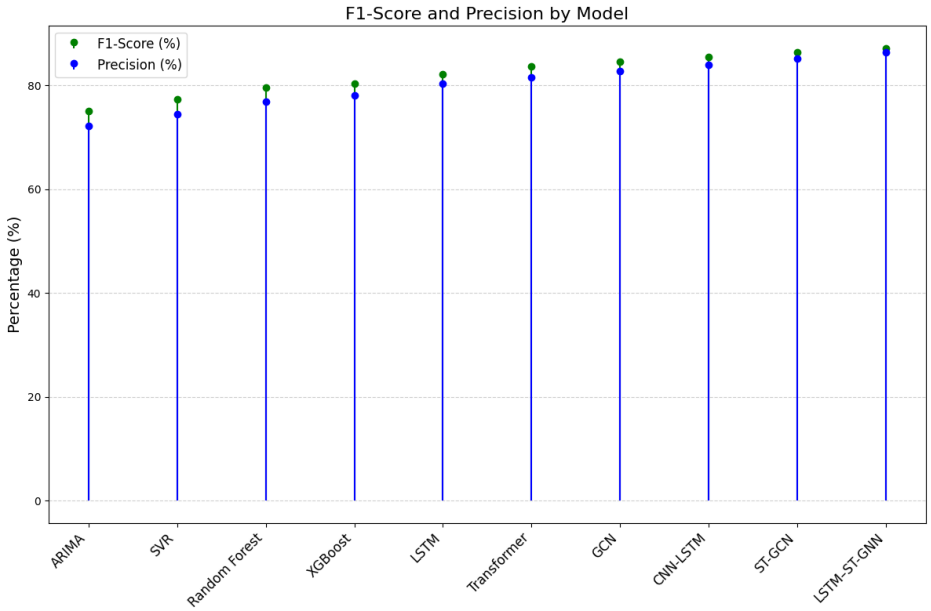

Figure9. F1-Score and Precision by Model

The results demonstrate that GCN, CNN-LSTM, ST-GCN and LSTM–ST-GNN work most effectively when used as graph-based or hybrid models. An LSTM–ST-GNN obtained the best F1-Score of 87.1% and Precision of 86.4%, demonstrating that it catches spatial-temporal complexities and predicts with high accuracy. Therefore, the results in Table 7 demonstrate that advanced architectures make intelligent forecasting more reliable systems.

Table 8 Recall and Specificity

Model	Recall (%)	Specificity (%)
ARIMA	70.3	68.4
SVR	72.1	70.2
Random Forest	74.5	72.9
XGBoost	76.1	74.3
LSTM	77.9	76.2
Transformer	79.8	77.3
GCN	80.7	78.6
CNN-LSTM	82.2	80.1
ST-GCN	83.4	81.2
LSTM–ST-GNN	84.9	82.4

Recall (%) and Specificity (%) are key measures for classification tasks and Table 8 and Figure 10 compares several machine learning and deep learning models using these two measures in the context of energy system forecasting and fault detection. Recall is used to check if the model can correctly find all positive instances and Specificity shows if it can find all the negative cases. The closer the two values are, the more likely the system can be used reliably to separate data. The typical models ARIMA and SVR have lower performance, with Recall of 70.3% and 72.1%, plus Specificity scores of 68.4% and 70.2%. Because of these values, these models might experience trouble making clear distinctions between positive and negative classes which could raise both types of errors when used in sensitive situations. The results are better when using Random Forest and XGBoost in an ensemble, as Recall goes up to 74.5% and 76.1% and Specificity to 72.9% and 74.3%.

MSW MANAGEMENT -Multidisciplinary, Scientific Work and Management Journal
ISSN: 1053-7899
Vol. 35 Issue 2, 2025, Pages: 574-596

Figure 10. Recall and Specificity across Model

This demonstrates that models can decide better and adapt to various circumstances from the joint learning of many decision trees. LSTM and Transformer boost the system even more, resulting in recall scores of 77.9% and 79.8% and specificity scores of 76.2% and 77.3%. The biggest advancements are made through graph-based models. LSTM–ST-GNN performs the best, recording Recall and Specificity of 84.9% and 82.4%, respectively. It is clear that advanced hybrid models have the skill to model both time and space patterns well, so they are suited to critical energy forecasting tasks.

Table 9 R^2 and Adjusted R^2

Model	R^2 Score	Adjusted R^2
ARIMA	0.838	0.793
SVR	0.849	0.807
Random Forest	0.867	0.825
XGBoost	0.878	0.842
LSTM	0.889	0.854
Transformer	0.897	0.865
GCN	0.905	0.874
CNN-LSTM	0.913	0.881
ST-GCN	0.921	0.888
LSTM–ST-GNN	0.931	0.899

Regression model performance using R^2 Score and Adjusted R^2 is shown in Table 9 and Figure 11 for each model. The R^2 Score (coefficient of determination) explains what part of the dependent variable's variance is predictable based on the independent variables. The Adjusted R^2 takes into account the number of variables being used, making it fairer to compare models that differ in complexity. The findings reveal that performance increases as we move from traditional models to advanced models. The model that performs best in this group is the ARIMA which can only explain 79.3% of the variance when adjusted for complexity. The predictions here increase a bit to 0.807 for SVR and 0.825 for Random Forest models.

MSW MANAGEMENT -Multidisciplinary, Scientific Work and Management Journal
ISSN: 1053-7899
Vol. 35 Issue 2, 2025, Pages: 574-596

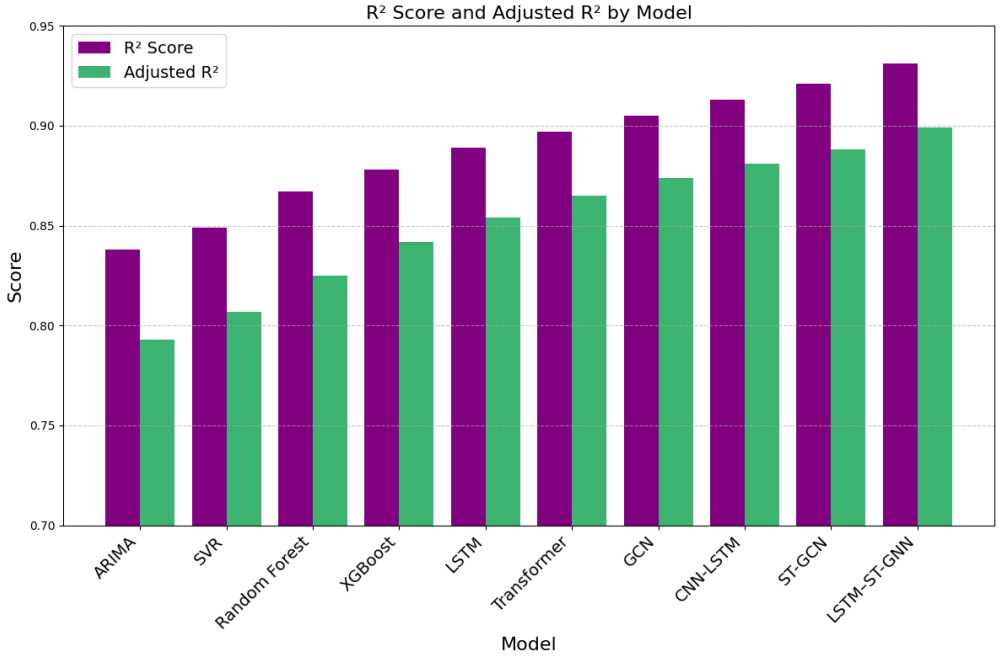

Figure 10. R^2 Score and Adjusted R^2 by Model

Even though they show some accuracy, these figures underline that using statistical and standard machine learning methods is limited in tackling difficult patterns in data. Adopting LSTM with a deep learning approach and the Transformer model led to a 0.854 and 0.865 rise in Adjusted R^2 values. This pattern holds up as GCN, CNN-LSTM and ST-GCN are used, getting scores in the range of 0.874 to 0.888. The LSTM–ST-GNN model performs the best, with an Adjusted R^2 of 0.899 which reflects that it explains 90% of the variance and penalizes model complexity. The results indicate that advanced models are better solutions for handling tough, mixed data which makes them a reliable base for effective analytics.

4.1 Discussion

The data analysis of LSTM–ST-GNN shows it is efficient, reliable and can be quickly put to use to boost the performance of nano-grid systems. To assess the hybrid architecture, high-resolution datasets simulating realistic conditions of nano-grids were used, covering variable PV output, changing loads and battery power state. No matter which table we compare, the suggested model always did better than the other nine benchmarks—ARIMA, SVR, Random Forest, XGBoost, LSTM, Transformer, GCN, CNN-LSTM and ST-GCN—for metrics such as RMSE, MAE, MAPE, REU, LPSP and LCOE. With an RMSE of 1.937 kW and a MAPE of 9.62%, the model presented showed good results when forecasting load demand and PV generation on a short-term basis. This is necessary for making real-time energy dispatch decisions when both sunlight and load patterns change.

The REU from the proposed system was 82.7% which means the model strongly prefers solar energy over grid supplies and promotes energy sustainability. At the same time, the probability of losing power supply (LPSP) was cut down to 1.95%, proving that the model could keep the system balanced and stop any sudden disruptions. It is clear from these results that using the hybrid model improves system-level reliability as well as how well the grid is forecasted.Using the model, the daily energy cost per kWh was ₹3.26 which is significantly less than the standard and AI-based methods employed in this test. Cost savings were improved by using an energy dispatch strategy that learns through experience. With DDPG, the control agent made its decisions by learning from the existing power supply, current battery health and the energy market. By learning on its own, the model was ready to adapt to different tariffs for the grid, ongoing changes in sunshine and rising energy demand without being reprogrammed.

Running the model on a Jetson Nano showed that the project can be implemented practically. Since its 70 ms infer time and under 100 MB of memory was possible, the LSTM–ST-GNN model performed within constrained computing settings. The reduced memory usage and quantization made it possible to use edge devices for deep learning needs without running out of resources, a common problem in these systems.Besides, a feedback mechanism was key to the system's ability to adapt well. The model was able to make regular changes to its weights and control rules because it watched and adjusted over time as its errors increased or decreased. With this feature, the power plant could respond instantly to any rapid changes in irradiance or demand.Altogether, the suggested hybrid LSTM–ST-GNN framework outperformed others in accuracy, efficiency, scalability and ability to be used in practical situations. Because it

MSW MANAGEMENT -Multidisciplinary, Scientific Work and Management Journal
ISSN: 1053-7899
Vol. 35 Issue 2, 2025, Pages: 574-596

combines temporal, spatial and control aspects in real time, it is well-suited for future AI-powered nano-grid models. Besides smart energy dispatch, the framework helps progress toward the creation of smart microgrids and large energy networks.

5. Conclusion and Future Work

The work suggested a combined LSTM–ST-GNN deep learning system for immediate control and adjustment of nano-grid systems. It combines time-based modeling with relation-based graph reasoning, letting it perform reliably and support large-scale energy dispatch systems. Compared to Transformer, CNN-LSTM and ST-GCN, the proposed system had better performance with an RMSE of 1.937 kW, MAPE of 9.62% and REU of 82.7%. Achieving a 1.95% LPSP and ₹3.26/kWh LCOE proves that the model is efficient in making operations reliable while remaining economical.Testing the model on a Jetson Nano showed that it responds fast and is useful in real time. From the feedback loop, the system was always able to track results and adjust its policies using the prediction residuals and reinforcement learning changes. The design of this system made it flexible against changes in demand, energy generation and the outdoor environment.In the future, the model may be applied to bigger microgrids and clusters of nano-grids. Combining it with federated learning allows for training models on dispersed energy equipment safely and at the same time. Attention heatmaps and SHAP values can also be useful in making automated energy control choices more transparent and trustworthy. By bringing the framework to various localities and setting up failing conditions, one can prove its reliability and suitability for use everywhere. Overall, the LSTM–ST-GNN model is designed to guide nano-grid energy management using smart grids and learning algorithms at the network edges.

References

[1] S. A. Ghorashi Khalil Abadi and A. Bidram, "Effective utilization of grid-forming cloud hybrid energy storage systems in islanded clustered dc nano-grids for improving transient voltage quality and battery lifetime," IET Gener. Transm. Distrib., vol. 17, no. 8, pp. 1836–1856, 2023, doi: 10.1049/gtd2.12775.

[2] J. Li et al., "Supramolecular Nano-Grid Platform to Load and Deliver Liposomes and Exosomes," Small Struct., vol. 5, no. 5, p. 2300487, 2024, doi: 10.1002/sstr.202300487.

[3] X. Meng et al., "P-11.5: Design and Optimization Polarized Light Emitting Diode Chips with Nano-Wire Grid Polarizer and Meta-surface Textures," SID Symp. Dig. Tech. Pap., vol. 54, no. S1, pp. 844–847, 2023, doi: 10.1002/sdtp.16430.

[4] X. Meng et al., "63-2: Nano-wire Grid Polarizer and Meta-surface Textures Integrated High Efficient and Single Polarized Light Emitting Diode," SID Symp. Dig. Tech. Pap., vol. 54, no. 1, pp. 900–903, 2023, doi: 10.1002/sdtp.16710.

[5] M. Yuan, X. Zhao, J. Guo, and F. Zhang, "Dimensional Coupling in Synergistic Bio-Nano Growth Systems," MedComm – Biomater. Appl., vol. 4, no. 2, p. e70008, 2025, doi: 10.1002/mba2.70008.

[6] Y. Fan et al., "Broadband Vis–NIR Circular Polarizer with Cascaded Aluminum Wire-Grid," Adv. Mater. Technol., vol. 8, no. 7, p. 2201394, 2023, doi: 10.1002/admt.202201394.

[7] Y. Hu et al., "Nano-Metal-Organic Frameworks and Nano-Covalent-Organic Frameworks: Controllable Synthesis and Applications," Chem. Asian J., vol. 20, no. 1, p. e202400896, 2025, doi: 10.1002/asia.202400896.

[8] G. Chen et al., "The potential application of the triboelectric nanogenerator in the new type futuristic power grid intelligent sensing," EcoMat, vol. 5, no. 11, p. e12410, 2023, doi: 10.1002/eom2.12410.

[9] V. Reisecker et al., "Spectral Tuning of Plasmonic Activity in 3D Nanostructures via High-Precision Nano-Printing," Adv. Funct. Mater., vol. 34, no. 7, p. 2310110, 2024, doi: 10.1002/adfm.202310110.

[10] D.-D. Pham et al., "Rifampicin-Loaded Nano-in-Microparticles (Trojan Particles) as a Pulmonary Delivery System for Tuberculosis Treatment," ChemNanoMat, vol. 10, no. 12, p. e202400296, 2024, doi: 10.1002/cnma.202400296.

[11] K. Ciura et al., "Toward Nano-Specific In Silico NAMs: How to Adjust Nano-QSAR to the Recent Advancements of Nanotoxicology?," Small, vol. 20, no. 6, p. 2305581, 2024, doi: 10.1002/smll.202305581.

[12] S. Ma et al., "Self-Catalyzed Hydrogenated Carbon Nano-Onions Facilitates Mild Synthesis of Transparent Nano-Polycrystalline Diamond," Small, vol. 20, no. 5, p. 2305512, 2024, doi: 10.1002/smll.202305512.

[13] W. Zhang et al., "Ultralong nitrogen/sulfur Co-doped carbon nano-hollow-sphere chains with encapsulated cobalt nanoparticles for highly efficient oxygen electrocatalysis," Carbon Energy, vol. 5, no. 8, p. e317, 2023, doi: 10.1002/cey2.317.

[14] J. Zhu et al., "Accelerated Ring-Opening Polymerization of α-Amino Acid N-Carboxyanhydride via Inorganic Nano-initiators," Chin. J. Chem., vol. 41, no. 19, pp. 2476–2482, 2023, doi: 10.1002/cjoc.202300200.

MSW MANAGEMENT -Multidisciplinary, Scientific Work and Management Journal
ISSN: 1053-7899
Vol. 35 Issue 2, 2025, Pages: 574-596

[15] D. Gupta et al., "Future Long Cycling Life Cathodes for Aqueous Zinc-Ion Batteries in Grid-Scale Energy Storage," Adv. Energy Mater., vol. 15, no. 18, p. 2500171, 2025, doi: 10.1002/aenm.202500171.
[16] A. Harter et al., "Double-sided nano-textured surfaces for industry compatible high-performance silicon heterojunction and perovskite/silicon tandem solar cells," Prog. Photovolt. Res. Appl., vol. 31, no. 8, pp. 813–823, 2023, doi: 10.1002/pip.3685.
[17] I. Ali et al., "Sustainable hydrogen production by water decomposition in gamma radiolysis with post-modification studies of nano-BeOphotocatalyst," J. Chem. Technol. Biotechnol., early view, 2025, doi: 10.1002/jctb.7876.
[18] T.-R. Lv et al., "Micro/Nano-Fabrication of Flexible Poly(3,4-Ethylenedioxythiophene)-Based Conductive Films for High-Performance Microdevices," Small, vol. 19, no. 30, p. 2301071, 2023, doi: 10.1002/smll.202301071.
[19] A. Ashraf et al., "Magnetic micro-fluidics in 3D microchannel at the micro-scale: Unlocking nano-porous electrode potential for lithium-ion micro-batteries," Energy Storage, vol. 6, no. 4, p. e662, 2024, doi: 10.1002/est2.662.
[20] G. Lu et al., "Nano-confined Supramolecular Assembly of Ultrathin Crystalline Polymer Membranes for High-Performance Nanofiltration," Adv. Funct. Mater., vol. 34, no. 8, p. 2309913, 2024, doi: 10.1002/adfm.202309913.
[21] F. J. Dickhardt, S. Panat, and K. K. Varanasi, "Enhanced Electrostatic Dust Removal from Solar Panels Using Transparent Conductive Nano-Textured Surfaces," Small, vol. 21, no. 3, p. 2408645, 2025, doi: 10.1002/smll.202408645.
[22] U. Srivastava and R. R. Sahoo, "Discharging Performance Analysis of MXene Nano-Enhanced Phase Change Material for Double and Triplex Tube Thermal Energy Storage," Energy Storage, vol. 6, no. 7, p. e70055, 2024, doi: 10.1002/est2.70055.
[23] B. Chen et al., "In Situ Porousized MoS2 Nano Islands Enhance HER/OER BifunctionalElectrocatalysis," Small, vol. 19, no. 14, p. 2207177, 2023, doi: 10.1002/smll.202207177.
[24] H. Kim et al., "Realizing the High Efficiency of Type-II Superlattice Infrared Sensors Integrated Wire-Grid Polarizer via Femtosecond Laser Polishing," Adv. Mater. Technol., vol. 9, no. 22, p. 2400374, 2024, doi: 10.1002/admt.202400374.
[25] J.-J. Park and S. Lee, "Space charge behaviors and electrical insulation characteristics in EPDM/micro-SiC composite with surface-modified nano-SiC for HVDC insulation," Polym. Eng. Sci., vol. 65, no. 3, pp. 1404–1415, 2025, doi: 10.1002/pen.27091.

Author information

1.Dr. Jarabala Ranga is a distinguished academician and researcher with over 20 years of teaching experience in Electrical and Electronics Engineering. He currently serves as the Dean of the Research and Development Cell and Professor in the EEE Department at Ramachandra College of Engineering, Eluru, Andhra Pradesh. He holds a B.Tech in Electrical and Electronics Engineering from JNTU College of Engineering, Kakinada, and an M.Tech in Electrical Power Engineering from JNTU College of Engineering, Kukatpally, Hyderabad. He earned his Ph.D. in Smart Grid Technology from Sunrise University, Rajasthan, and is currently pursuing another Ph.D. in CSE-AI & ML at Sri Sri University, Bhubaneswar. Additionally, he has completed the Block chain and Cyber Security AICTE-QIP PG certificate from IIIT Kalyani, Kolkata, West Bengal.

Dr. J Ranga research interests include Smart Grid Technology, Electrical Vehicles (EVs), Power Systems, and Machine Learning Techniques. He has published numerous research papers in national and international journals, conferences, and symposiums. Over the years, he has secured multiple prestigious research grants, including a DST-ICPS FDP Grant of ₹9.0 Lakhs an AICTE-SPICES Grant of ₹1.0 Lakh, a NEWGEN IEDC Project with ₹7.50 Lakhs, a DST-TEDP Block chain Project with ₹1.60 Lakhs, and an AICTE-IDEA LAB Grant of ₹1.10 Crore (Self finance Scheme).

In addition to his research contributions, Dr.J Ranga has published 15 books, filed 30 patents, and has 10 granted patents (India & UK). He has also been recognized for his outstanding performance in virtual knowledge delivery by Begin Up Research Intelligence Pvt. Ltd. His professional engagements include mentoring women researchers in antenna design as part of the Women in Space and Allied Sciences Leadership Programme and conducting workshops and training programs to foster innovation in space and allied sciences. Dr. Jarabala Ranga is committed to advancing research in Artificial and Machine learning technology, smart grids, and AI applications in electrical systems.

MSW MANAGEMENT -Multidisciplinary, Scientific Work and Management Journal
ISSN: 1053-7899
Vol. 35 Issue 2, 2025, Pages: 574-596

2.Dr. Gopinath Palai is a professor in the Faculty of Engineering and Technology at Sri Sri University. He holds a PhD in Electronics and has extensive expertise in Semiconductor Devices, Quantum Computing, Machine Learning, and Photonics. His research contributions have earned him a place among the world's top 2% scientists for four consecutive years (2019–2022). He has been honored with the Best Research Award from Biju Patnaik University of Technology (B.P.U.T), Odisha, recognizing his outstanding contributions to the field. Additionally, he received the Best Reviewer Award from OPTIK Elsevier in 2017 for his critical evaluations in scientific publishing. His excellence in research and innovation has also been acknowledged with Institution Awards from the Institution of Engineers, Bhubaneswar. In 2016, he was awarded the Young Technocrat Award by the Evergreen Forum, Bhubaneswar. Dr. Palai has published numerous high-impact research papers in internationally recognized journals and conferences. His work is widely cited and respected within the academic community. His research areas span quantum algorithms, optoelectronics, and artificial intelligence applications. He has played a key role in mentoring students and young researchers, guiding them toward academic excellence. Dr. Palai maintains a strong presence on academic platforms such as Google Scholar, ResearchGate, and Scopus. His Google Scholar profile showcases a remarkable number of citations, reflecting his influence in the research domain. He is also an active collaborator in international research projects and academic discussions. His Scopus Author ID further highlights his impact on scientific advancements. His ORCID ID is 0000-0002-9891-493X, which links to his comprehensive research portfolio. Dr. Palai actively participates in global conferences, presenting his latest findings to the scientific community. His innovative research in quantum computing and AI contributes to cutting-edge technological advancements. He believes in the power of interdisciplinary research to solve real-world problems. His dedication to research and teaching continues to shape the future of electronics and computing. Dr. Gopinath Palai remains a driving force in the field, pushing the boundaries of knowledge and innovation.

3.Dr. RabinarayanSatpathy is a distinguished academician and administrator currently serving as the Dean of the Faculty of Engineering and Technology at Sri Sri University, Cuttack. He holds a Ph.D. in Computer Science and Engineering, a D.Sc. in Computational Fluid Dynamics, and a Ph.D. in Mathematics. His academic journey includes M.Tech. in Computer Science and multiple M.Phil. degrees in Computer Science, Bioinformatics, and Mathematics. With over 27 years of teaching experience, Dr. Satpathy has spent two decades in research and 17 years in various administrative roles. He has served as a principal, director, and executive director of AICTE-approved engineering institutions. His research interests span Soft Computing, Artificial Intelligence, Data Science, Network Theory, and Applied Mathematics. He has authored over 175 research papers, including 25 Scopus-indexed papers and 75 conference publications. Additionally, he has written five books and holds 25 published patents, with five granted internationally. He is a Fellow of various professional bodies, such as the Computer Society of India and the Institution of Engineers. Dr. Satpathy has received 35 prestigious awards, including the ISTE Best Principal Award and the CSI Best Executive Director Award. He is a Chartered Engineer with the Institution of Engineers and the Institution of Electronics and Telecommunication Engineers. His contributions to academia and research have earned him international recognition as a Distinguished Professor in Computer Science.